

Optimizing ^{66}Ga Yields: Evaluating Production Routes via Proton, ^3He and Alpha Particles Bombardment of Copper and Zinc Isotopes

 Susan Shukur Noori *



Department of Physics, College of Science, University of Kirkuk, Kirkuk, Iraq.

*Corresponding author : [✉ susannoori@uokirkuk.edu.iq](mailto:susannoori@uokirkuk.edu.iq)

Article Information

Article Type:

Research Article

Keywords:

Gallium-66 production; Nuclear cross sections; TALYS calculations; Medical isotope production; PET imaging isotopes.

History:

Received: 14 January 2025

Revised: 2 March 2025

Accepted: 3 March 2025

Available Online: 13 March 2025

Citation: Susan Shukur Noori, Optimizing ^{66}Ga Yields: Evaluating Production Routes via Proton, ^3He and Alpha Particles Bombardment of Copper and Zinc Isotopes, Kirkuk Journal of Science, 20(1), p. 23-34, 2025, <https://doi.org/10.32894/kujss.2025.156644.1192>

Abstract

The medium-lived radionuclide Gallium-66 ($T_{1/2} = 9.5$ hours, $\beta^+ = 56\%$, and $\varepsilon = 45\%$) plays a crucial role in positron emission tomography (PET). This study comprehensively analyzes twelve distinct nuclear reaction pathways for ^{66}Ga production, examining proton, helium-3, and alpha particle bombardment on copper and zinc targets. Cross sections were calculated using the TALYS 1.9 nuclear reaction simulation code for reactions including $^{66}\text{Zn}(p, n)^{66}\text{Ga}$, $^{67}\text{Zn}(p, 2n)^{66}\text{Ga}$, $^{68}\text{Zn}(p, 3n)^{66}\text{Ga}$, $^{nat}\text{Zn}(p, x)^{66}\text{Ga}$, $^{65}\text{Cu}(^3\text{He}, 2n)^{66}\text{Ga}$, $^{nat}\text{Cu}(^3\text{He}, x)^{66}\text{Ga}$, $^{66}\text{Zn}(^3\text{He}, x)^{66}\text{Ga}$, $^{nat}\text{Zn}(^3\text{He}, x)^{66}\text{Ga}$, $^{63}\text{Cu}(a, n)^{66}\text{Ga}$, $^{65}\text{Cu}(a, 3n)^{66}\text{Ga}$, $^{nat}\text{Cu}(a, x)^{66}\text{Ga}$ and $^{64}\text{Zn}(a, x)^{66}\text{Ga}$. The investigation encompassed both natural and enriched isotope targets (^{63}Cu , ^{65}Cu , ^{nat}Cu , ^{64}Zn , ^{66}Zn , ^{67}Zn , ^{68}Zn , and ^{nat}Zn), with theoretical calculations validated against experimental data from the EXFOR library. Notably, the $^{66}\text{Zn}(p, n)^{66}\text{Ga}$ and $^{64}\text{Zn}(a, x)^{66}\text{Ga}$ reactions demonstrated exceptional efficiency, achieving peak cross sections of 400-440 mb and 600-640 mb respectively. For each reaction pathway, optimal energy ranges, threshold energies, and Q-values were determined, providing essential parameters to optimize ^{66}Ga production in medical applications.

1. Introduction:

Nuclear cross-sections offer fundamental insight into the probability of nuclear reactions and form a bedrock in the understanding of nuclear physics and its applications. Thus, even though nuclear reaction studies have undergone remarkable development, it is still lack an understanding of the nature of chemical reaction dynamics. This disparity gives challenges and opportunities to researchers working in nuclear physics and its applications. Gallium isotopes have very successfully established themselves in nuclear medicine for more than five decades. Versatile isotopes have been of utmost importance in

diagnostic imaging and therapeutic interventions, especially in cancers, bone disorders, and calcium-related disorders. Radiation therapy is one such modality employing ionizing radiation targeting malignant cells and has become the cornerstone in the modern cancer treatment protocol. Among the different gallium isotopes, special interest has been attracted by the ^{66}Ga isotope, due to specific properties making it highly suitable for PET imaging. The increasing significance of PET in contemporary medical diagnostics, combined with the unique properties of ^{66}Ga as a positron emitter for tumor imaging, serves as the foundation for this comprehensive study [1], [2], [3] and [4].

Our theoretical calculation methodology for nuclear reaction cross sections will involve multiple particle types such as protons, Helium-3, and alpha particles interacting with copper and zinc isotopes using the sophisticated Monte Carlo nuclear reaction simulation code TALYS 1.9. To validate our theo-

3005-4788 (Print), 3005-4796 (Online) Copyright © 2025. This is an open access article distributed under the terms and conditions of the Creative Commons Attribution (CC-BY 4.0) license (<https://creativecommons.org/licenses/by/4.0/>)



retical findings, we executed systematic comparisons with the experimental data available from the EXFOR database [5], providing a way of quantifying the observed discrepancies between theoretical predictions and the corresponding experimental findings. The growing need for medical radioisotopes is increasing pressure to arrive at more effective production routes for clinically relevant isotopes. ^{66}Ga has become a very important radioisotope in this respect because it possesses special advantages in the PET imaging of slow biological processes, for example, lymphatic transport and tumor metabolism. Its half-life of 9.49 hours is extremely suitable for most applications in medical imaging and allows an ideal compromise between the practical handling time and the effective delivery of a radiation dose. The twelve investigated nuclear reactions could provide alternative methods for the production of ^{66}Ga . The investigation addresses both the natural targets ^{nat}Cu and ^{nat}Zn and the enriched isotopes ^{63}Cu , ^{65}Cu , ^{64}Zn , ^{66}Zn , ^{67}Zn , and ^{68}Zn , which allows one to compare different production strategies. Every reaction pathway is determined by specific energy requirements, threshold values, and Q-values that may give important information in the optimization of the production protocols. The excitation functions of these reactions show quite different cross-sectional behaviors. The most important among them is the $^{66}\text{Zn}(p,n)^{66}\text{Ga}$ reaction, which presents favorable characteristics due to its high cross sections in the medium energy range. Similar options also exist for $^{64}\text{Zn}(a,x)^{66}\text{Ga}$; in particular, interesting complementarities with higher energies might be established that could form complementary production routes. This paper extends considerations to aspects of radioisotope production practice in depth, with details of target material, energy optimization, and yield prediction. The compilation of cross-sectional data with the theoretical calculations gives the necessary insight into facility planning and the elaboration of effective protocols of production.

The theoretical framework of this study is based on previous research using Monte Carlo methods, as represented in several studies during the last decade. These prior investigations have established the validity of computational approaches in predicting nuclear reaction outcomes and have helped identify areas where theoretical models require refinement. The significance of this research extends beyond academic interest, addressing practical challenges in medical radioisotope production. In this work, some production routes of ^{66}Ga were deeply analyzed with the aim of contributing to the optimization of its production for clinical applications. The obtained results will have direct consequences on the medical facilities that intend to create or upgrade their radioisotope production capabilities. Theoretical calculations with the subsequent validation by means of experimental data are a good approach to the understanding of nuclear reaction mechanisms. This methodology identifies not only the most promising production routes but also indicates where

refinement of theoretical models is necessary. Systematic comparison with experimental data will ensure that our conclusions have a basis in practical reality while taking further steps in theoretical understanding.

This work forms the basis for future studies into radioisotope production optimization. The comprehensive investigation of various reaction pathways, including practical considerations for implementation in production, provides a very useful knowledge base for the nuclear medicine community. As the need for medical radioisotopes grows, such detail-oriented studies will be increasingly needed to ensure effective and reliable methods of production. Other investigations in this field have also been performed via Monte Carlo methods [6], [7], [8], [9] and [10].

2. Material and Methods:

The production of radioactive isotopes requires precise control and understanding of nuclear reactions. This study focuses on determining optimal projectile energy ranges to maximize radioisotope yields through both theoretical calculations and experimental validation [11], [12]. Our research specifically examines the cross sections for Gallium production via proton, Helium-3, and alpha particle induced nuclear reactions on Copper and Zinc targets. In our investigation utilizes several target materials commonly employed in ^{66}Ga radioisotope production:

1. Copper isotopes: ^{63}Cu , ^{65}Cu , and natural copper (^{nat}Cu).
2. - Zinc isotopes: ^{64}Zn , ^{66}Zn , ^{67}Zn , ^{68}Zn , and natural zinc (^{nat}Zn).

These target materials were selected based on their established role in producing ^{66}Ga , a radioisotope crucial for nuclear medicine applications, particularly in studying slow dynamic processes such as lymphatic transport through positron emission tomography. The study encompasses twelve distinct nuclear reactions: Proton-induced reactions: $^{66}\text{Zn}(p,n)^{66}\text{Ga}$, $^{67}\text{Zn}(p,2n)^{67}\text{Ga}$, $^{68}\text{Zn}(p,3n)^{66}\text{Ga}$, $^{nat}\text{Zn}(p,x)^{66}\text{Ga}$. Helium-3-induced reactions: $^{65}\text{Cu}(^3\text{He},2n)^{66}\text{Ga}$, $^{nat}\text{Cu}(^3\text{He},x)^{66}\text{Ga}$, $^{66}\text{Zn}(^6\text{He},x)^{66}\text{Ga}$, $^{nat}\text{Zn}(3\text{He},x)^{66}\text{Ga}$. And Alpha particle-induced reactions: $^{63}\text{Cu}(a,n)^{66}\text{Ga}$, $^{65}\text{Cu}(a,3n)^{66}\text{Ga}$, $^{nat}\text{Cu}(a,x)^{66}\text{Ga}$, $^{64}\text{Zn}(a,x)^{66}\text{Ga}$.

All theoretical calculations were performed using TALYS 1.9 code, an advanced Monte Carlo simulation program. This computational tool offers several key capabilities:

1. Energy range coverage: 1 keV to 200 MeV.
2. Applicable to target nuclides with mass numbers ≥ 12 .
3. Handles multiple projectile types: neutrons, photons, protons, deuterons, tritons, ^3He , and alpha-particles.

4. Calculates total reaction cross-sections.
5. Determines values based on branching ratios across different reaction channels and mechanisms [13].

The program, implemented in FORTRAN and running on Linux operating systems, provides comprehensive analysis of nuclear reaction parameters. These calculations help establish the accuracy of various parameters that are also derived from experimental measurements, enabling validation through comparison with empirical data.

3. Results and Discussion:

The $^{66}\text{Zn}(p, n)^{66}\text{Ga}$, $^{67}\text{Zn}(p, 2n)^{66}\text{Ga}$, $^{68}\text{Zn}(p, 3n)^{66}\text{Ga}$, $^{nat}\text{Zn}(p, x)^{66}\text{Ga}$ for proton induced $^{65}\text{Cu}(\text{He}, 2n)^{66}\text{Ga}$, $^{nat}\text{Cu}(^3\text{He}, x)^{66}\text{Ga}$, $^{66}\text{Zn}(^3\text{He}, x)^{66}\text{Ga}$, $^{nat}\text{Zn}(^3\text{He}, x)^{66}\text{Ga}$ for helium-3 induced and $^{63}\text{Cu}(a, n)^{66}\text{Ga}$, $^{65}\text{Cu}(a, 3n)^{66}\text{Ga}$, $^{nat}\text{Cu}(a, x)^{66}\text{Ga}$, $^{64}\text{Zn}(a, x)^{66}\text{Ga}$ for alpha induced production reaction excitation functions were calculated theoretically using TALYS 1.9 code. We compared our theoretical results with experimental data from the EXFOR database.

3.1 Proton Induced Reactions:

The excitation functions for proton-induced reactions in Zinc nuclei were calculated theoretically using the TALYS 1.9 code. Four specific reactions were analyzed: $^{66}\text{Zn}(p, n)^{66}\text{Ga}$, $^{67}\text{Zn}(p, 2n)^{66}\text{Ga}$, $^{68}\text{Zn}(p, 3n)^{66}\text{Ga}$, and $^{nat}\text{Zn}(p, x)^{66}\text{Ga}$. The theoretical results were compared with experimental data and presented in Figures 1, 2, 3 and 4.

$^{66}\text{Zn}(p, n)^{66}\text{Ga}$ Reaction (Figure 1):

Our theoretical calculations for the $^{66}\text{Zn}(p, n)^{66}\text{Ga}$ nuclear reaction demonstrate strong consistency with existing experimental data across an energy range from below 10 MeV to above 30 MeV. In the peak region, experimental data from Szelecsenyi et al. (1998), Levkovski et al. (1991), and Hille et al. (1972) exceed our calculated results by approximately 25%. Conversely, data reported by Hermann et al. (1992) shows lower values than our calculations beginning at 12 MeV. The cross-section exhibits a pronounced peak around 10-15 MeV, reaching maximum values of approximately 600 mb for our calculations, followed by a sharp decrease approaching zero beyond 40 MeV.

$^{67}\text{Zn}(p, 2n)^{66}\text{Ga}$ Reaction (Figure 2):

For the $^{67}\text{Zn}(p, 2n)^{66}\text{Ga}$ reaction, our calculations show excellent agreement with experimental data from Szelecsenyi et al. (2003, 1998), particularly below 25 MeV where most experimental data is available. The results align especially well with data from Szelecsenyi et al. (1998), Levkovski (1991), and Tarkanyi et al. (1990) in the low-energy region up to 20 MeV, though their peak values exceed our calculations by 25%, 20%, and 10% respectively. The cross-section peaks

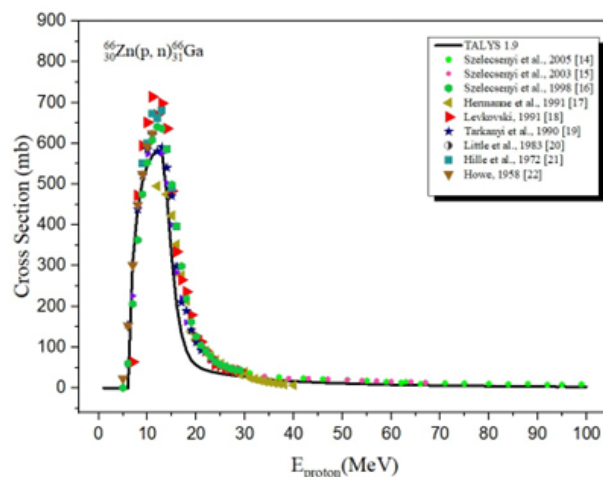


Figure 1. Our cross-section calculations of $^{66}\text{Zn}(p, n)^{66}\text{Ga}$ reaction compared with experimental data [14, 15, 16, 17, 18, 19, 20, 21, 22].

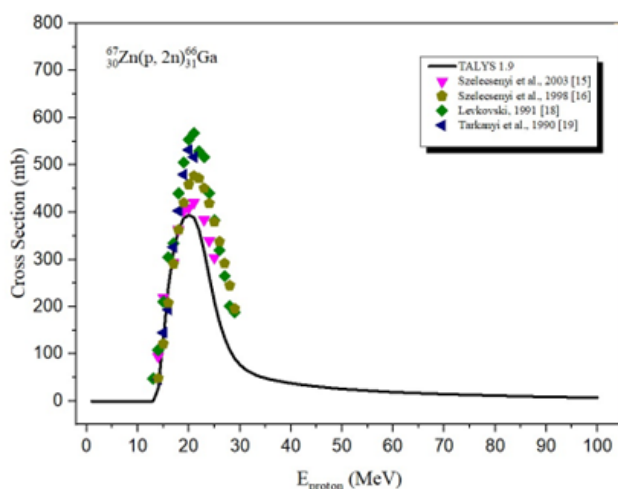


Figure 2. Our cross-section calculations of $^{67}\text{Zn}(p, 2n)^{66}\text{Ga}$ reaction compared with experimental data [15, 16, 18, 19].

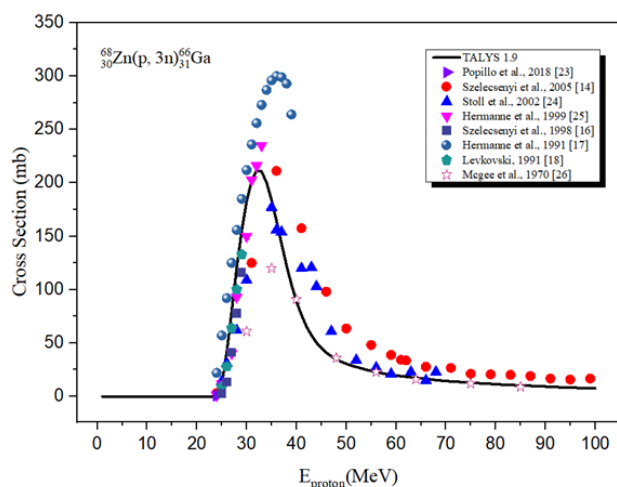


Figure 3. Our cross-section calculations of $^{68}\text{Zn}(p,3n)^{66}\text{Ga}$ reaction compared with experimental data [14], [16, 17, 18], [23, 24, 25, 26].

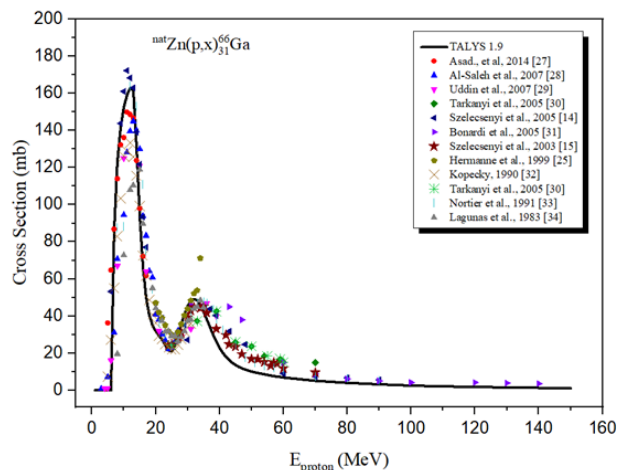


Figure 4. Our cross-section calculations of $^{nat}\text{Zn}(p,x)^{66}\text{Ga}$ reaction compared with experimental data [14], [15], [25], [27, 28, 29, 30, 31, 32, 33, 34].

around 20-25 MeV, reaching approximately 400 mb.

$^{68}\text{Zn}(p,3n)^{66}\text{Ga}$ Reaction (Figure 3):

The $^{68}\text{Zn}(p,3n)^{66}\text{Ga}$ reaction calculations show patterns consistent with experimental data from Szelecsenyi et al. (2005) and Stoll et al. (2002). Strong agreement is observed with data from Pupillo et al. (2018), Szelecsenyi et al. (1998), and Levkovski (1991) at energies up to 30 MeV. Hermann et al. (1999) data matches our results closely except for the final points, while Hermann et al. (1992) data exceeds our calculations by about 30% between 30-40 MeV. McGee et al. (1970) data shows strong agreement at energies above 40 MeV. The reaction exhibits a distinctive peak around 35-40 MeV, reaching approximately 200 mb for our calculations.

$^{nat}\text{Zn}(p,x)^{66}\text{Ga}$ Reaction (Figure 4):

The $^{nat}\text{Zn}(p,x)^{66}\text{Ga}$ reaction calculations reveal a complex pattern with two distinct peaks. The first peak occurs at 17 MeV, initiated by the $^{66}\text{Zn}(p,n)$ reaction contribution starting at 8 MeV. The $^{67}\text{Zn}(p,2n)$ reaction's influence causes a subsequent decrease in cross-section, while the $^{68}\text{Ga}(p,3n)$ reaction's contribution begins near 25 MeV, creating a second peak at 34 MeV. Our calculations generally align well with experimental literature, though some experimental points from Szelecsenyi et al. (2005), Bonardi et al. (2005), and Hermann et al. (1999) show slightly higher values than our calculations. The primary peak reaches approximately 170 mb at 12-15 MeV, while the secondary peak achieves about 45 mb at 35-40 MeV.

The comprehensive analysis of these proton-induced reactions provides valuable insights into the production mechanisms of ^{66}Ga , with theoretical calculations generally showing good agreement with experimental data across multiple studies and energy ranges. The observed variations between theoretical and experimental results, particularly in peak regions, contribute to our understanding of the reaction mechanisms and help refine production parameters for practical applications.

3.2 Helium-3 Induced Reactions:

Excitation functions for helium-3 induced reactions in Copper and Zinc nuclei were calculated using the TALYS 1.9 nuclear reaction simulation code. Four specific reactions were analyzed: $^{65}\text{Cu}(^3\text{He},2n)^{66}\text{Ga}$, $^{nat}\text{Cu}(^3\text{He},x)^{66}\text{Ga}$, $^{66}\text{Zn}(^3\text{He},x)^{66}\text{Ga}$, and $^{nat}\text{Zn}(^3\text{He},x)^{66}\text{Ga}$. These theoretical calculations were compared with experimental data from the EXFOR library which were plotted in Figures 5, 6, 7 and 8.

$^{65}\text{Cu}(^3\text{He},2n)^{66}\text{Ga}$ Reaction (Figure 5):

The theoretical calculations for the $^{65}\text{Cu}(^3\text{He},2n)^{66}\text{Ga}$ reaction show good agreement with experimental data from Misaelides et al. (1980), Golchert et al. (1970), and Lebowitz et al. (1970). However, significant discrepancies were ob-

served with data from Bissem et al. (1980) and Bryant et al. (1963). particularly at energies above 15 MeV, where their values exceed our calculations by approximately 40% and 20%, respectively. The cross-section peaks between 15-20 MeV, with experimental values reaching 370 mb compared to our theoretical prediction of 220 mb.

$^{nat}\text{Cu}(^3\text{He},x)^{66}\text{Ga}$ Reaction (Figure 6):

For the $^{nat}\text{Cu}(^3\text{He},x)^{66}\text{Ga}$ reaction, our theoretical results demonstrate excellent agreement with experimental data reported by Tarkanyi et al. (2002, 1992) in the energy range below 15 MeV. Beyond 16 MeV, experimental data shows values approximately 20% higher than our calculations. The cross-section exhibits a well-defined peak around 15-20 MeV, with experimental values reaching 90 mb while our calculations predict a maximum of about 65 mb.

$^{66}\text{Zn}(^3\text{He},x)^{66}\text{Ga}$ Reaction (Figure 7):

The theoretical calculated results for the $^{66}\text{Zn}(^3\text{He},x)^{66}\text{Ga}$ nuclear reaction was compared with experimental data available in literature. Only one study found in EXEOR library which performed by Nagame, et al. (1989). A good agreement between calculated results and experimental data to energy range up to 30 MeV with a small shift to the right in the peak region about 5 MeV for the experimental data. The maximum in the cross-section is reached around 35-40 MeV, with experimental values of about 550 mb, while our theoretical model predicts about 450 mb.

$^{nat}\text{Zn}(^3\text{He},x)^{66}\text{Ga}$ Reaction (Figure 8):

Analysis of the $^{nat}\text{Zn}(^3\text{He},x)^{66}\text{Ga}$ reaction shows good overall agreement between our theoretical calculations and the experimental data reported by Al-Abyad et al. (2017). The excitation function reveals distinctive features: a plateau beginning around 11 MeV due to the $^{64}\text{Zn}(^3\text{He},p)$ reaction contribution, followed by increased cross-sections above 15 MeV attributed to the $^{66}\text{Zn}(^3\text{He},x)$ reaction. The cross-section peaks at 30-35 MeV, reaching approximately 135 mb, with our calculations effectively reproducing both the shape and magnitude of the experimental excitation function. The comprehensive analysis of these helium-3 induced reactions provides valuable insights into ^{66}Ga production mechanisms. The generally good agreement between theoretical calculations and experimental data, despite some discrepancies in peak regions, validates the predictive capabilities of the TALYS 1.9 code for these reaction channels. Given the limited experimental data available for some reactions, particularly the $^{66}\text{Zn}(^3\text{He},x)^{66}\text{Ga}$ and $^{nat}\text{Zn}(^3\text{He},x)^{66}\text{Ga}$ reactions, our theoretical calculations offer important guidance for future experimental investigations.

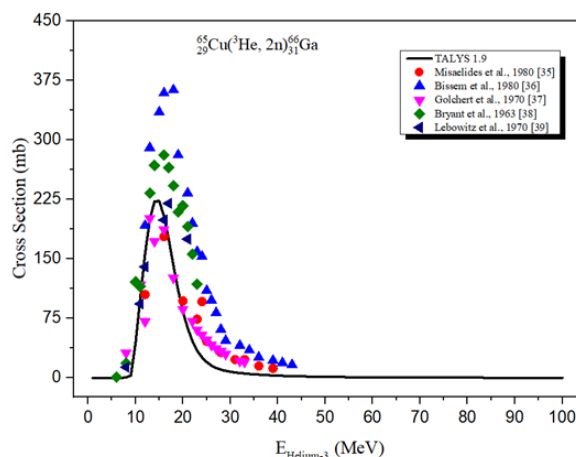


Figure 5. Our cross-section calculations of $^{65}\text{Cu}(^3\text{He},2n)^{66}\text{Ga}$ reaction compared with experimental data [35, 36, 37, 38, 39].

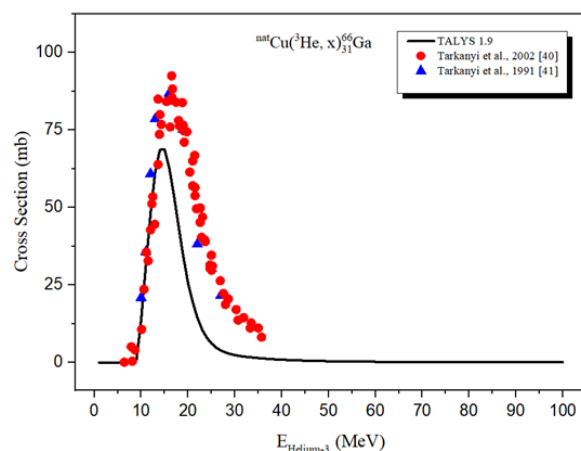


Figure 6. Our cross-section calculations of $^{nat}\text{Cu}(^3\text{He},x)^{66}\text{Ga}$ reaction compared with experimental data [40], [41].

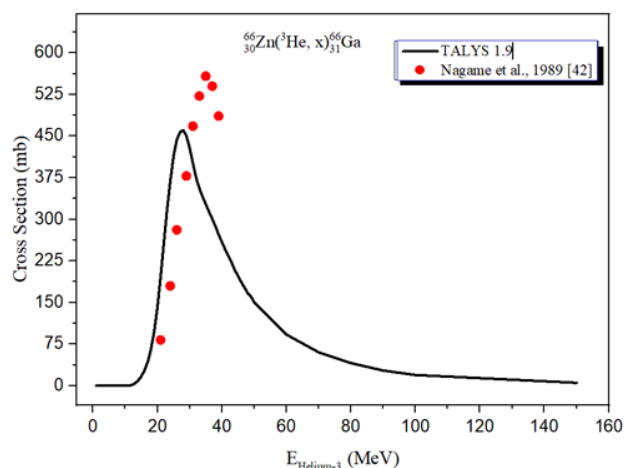


Figure 7. Our cross-section calculations of $^{66}\text{Zn} (^3\text{He}, x)^{66}\text{Ga}$ reaction compared with experimental data [42].

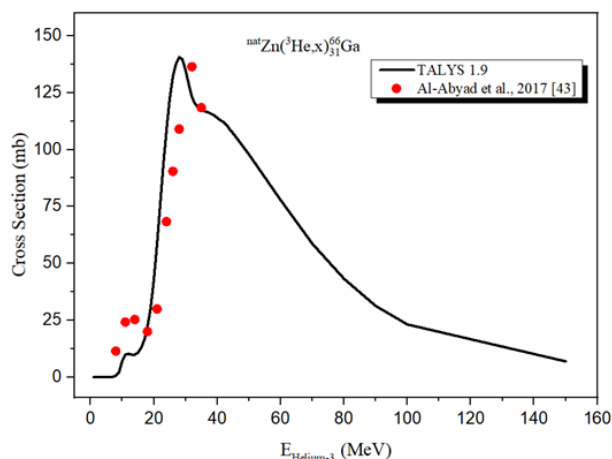


Figure 8. Our cross-section calculations of $^{nat}\text{Zn} (^3\text{He}, x)^{66}\text{Ga}$ reaction compared with experimental data [43].

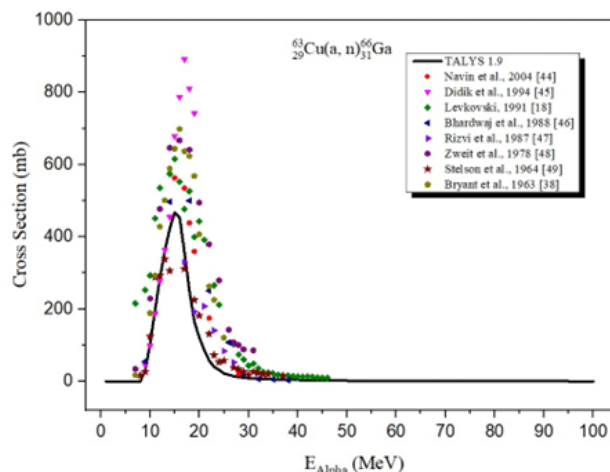


Figure 9. Our cross-section calculations of $^{63}\text{Cu} (a, n)^{66}\text{Ga}$ reaction compared with experimental data [18], [38], [44, 45, 46, 47, 48, 49].

3.3 Alpha Induced Reactions:

Theoretical excitation functions for alpha particle-induced reactions producing ^{66}Ga were calculated using the TALYS 1.9 code. Four specific reactions were analyzed: $^{63}\text{Cu}(a, n)^{66}\text{Ga}$, $^{65}\text{Cu}(a, 3n)^{66}\text{Ga}$, $^{nat}\text{Cu}(a, x)^{66}\text{Ga}$, and $^{64}\text{Zn}(a, x)^{66}\text{Ga}$. These calculations were compared with published experimental data from the EXFOR library as shown in Figures 9, 10, 11, 12.

$^{63}\text{Cu}(a, n)^{66}\text{Ga}$ Reaction Figure 9:

Our theoretical calculations for the $^{63}\text{Cu}(a, n)^{66}\text{Ga}$ reaction show varying degrees of agreement with experimental data. Results from Didik et al. (1994) match our calculations perfectly up to 14 MeV but exceed our predictions by a factor of two in the peak region. Data from Levkovski (1991), Zweit et al. (1987), and Bryant et al. (1963) consistently show higher cross-sections than our calculations, though the overall reaction behavior patterns remain compatible. The experimental data shows a pronounced peak between 15-20 MeV, reaching approximately 800 mb, while our calculations predict a maximum of about 450 mb.

$^{65}\text{Cu}(a, 3n)^{66}\text{Ga}$ Reaction Figure 10:

The $^{65}\text{Cu}(a, 3n)^{66}\text{Ga}$ reaction calculations demonstrate strong parallelism with experimental data from Levkovski (1991). Good agreement is also observed with results from Takacs et al. (2017), Didik et al., (1994) and Proges (1956), though experimental data beyond 37 MeV is lacking. The cross-section peaks around 45-50 MeV, reaching approximately 400 mb, with our theoretical predictions accurately capturing both peak position and magnitude.

$^{nat}\text{Cu}(a, x)^{66}\text{Ga}$ Reaction Figure 11:

Analysis of the $^{nat}\text{Cu}(a, x)^{66}\text{Ga}$ reaction reveals a distinc-

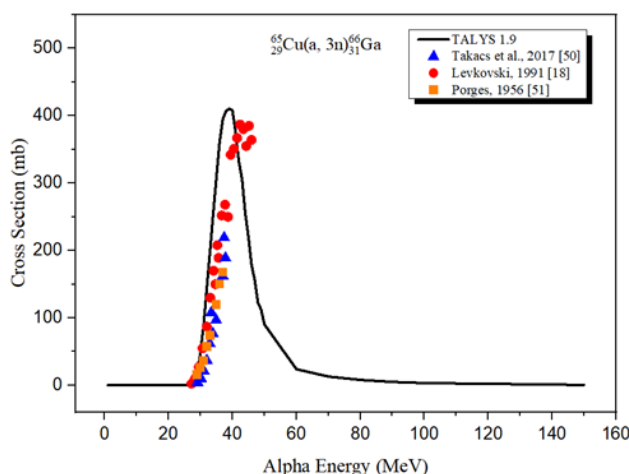


Figure 10. Our cross-section calculations of $^{65}\text{Cu}(a,3n)^{66}\text{Ga}$ reaction compared with experimental data [18], [50], [51].

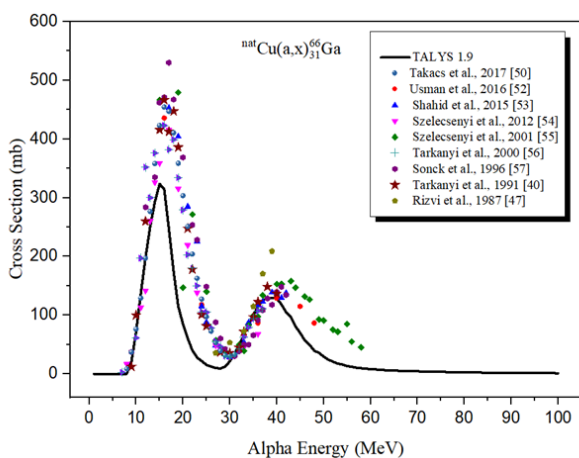


Figure 11. Our cross-section calculations of $^{nat}\text{Cu}(a,x)^{66}\text{Ga}$ reaction compared with experimental data [40], [47], [50], [52, 53, 54, 55, 56, 57].

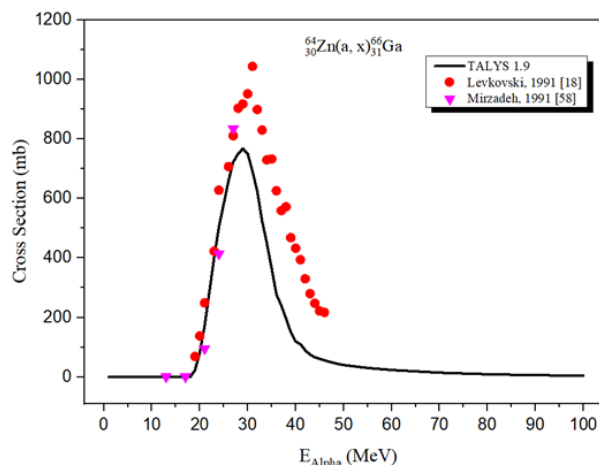


Figure 12. Our cross-section calculations of $^{64}\text{Zn}(a,x)^{66}\text{Ga}$ reaction compared with experimental data [18], [58].

tive double-peaked structure. The first peak, attributed to the $^{63}\text{Cu}(a,n)$ reaction, occurs at 15 MeV and extends to 28 MeV. The second peak at 40 MeV results from combined contributions of $^{63}\text{Cu}(a,n)$ and $^{65}\text{Cu}(a,3n)$ reactions, appearing at energies above 29 MeV. Our calculations show excellent agreement with published data, particularly in the low-energy region up to 14 MeV and between 30-42 MeV. The primary peak reaches approximately 320 mb, while the secondary peak achieves about 150 mb.

$^{64}\text{Zn}(a,x)^{66}\text{Ga}$ Reaction Figure 12:

The $^{64}\text{Zn}(a,x)^{66}\text{Ga}$ reaction calculations were compared with experimental data from Levkovski (1991) and Mirzadeh (1991). While Levkovski's data shows similar patterns to our calculations, their cross-sections are approximately 15% higher than our predictions. Our results align almost perfectly with Mirzadeh's data, except for their final data point. The reaction exhibits a pronounced peak around 30-35 MeV, with experimental values exceeding 1000 mb, while our calculations predict a maximum of approximately 750 mb.

These comprehensive analyses of alpha-induced reactions provide valuable insights into ^{66}Ga production mechanisms. The generally good agreement between theoretical calculations and experimental data, despite some discrepancies in peak magnitudes, validates the TALYS 1.9 code's predictive capabilities while highlighting areas where theoretical models might need refinement. The observed variations in cross-section magnitudes and peak positions across different studies emphasize the importance of continued experimental validation of theoretical predictions. The compilation presents comprehensive nuclear reaction parameters for various ^{66}Ga production routes using proton, helium-3, and alpha particle bombardment of zinc and copper targets. Two reactions stand out for their particularly high cross sections: $^{66}\text{Zn}(p,n)^{66}\text{Ga}$

Table 1. Optimum energy range, the average cross section of these energies, E-threshold and Q-values for ^{66}Ga production.

Reactions	Optimum energy range (MeV)	Average cross Section(mb)	E-threshold (MeV)	Q-values (MeV)
$^{66}\text{Zn}(p, n)^{66}\text{Ga}$	$E_p = 8 \rightarrow 15$	400 \rightarrow 440	6.09286	-5.95735
$^{67}\text{Zn}(p, 2n)^{66}\text{Ga}$	$E_p = 17 \rightarrow 23$	320 \rightarrow 360	13.2055	-13.0097
$^{68}\text{Zn}(p, 3n)^{66}\text{Ga}$	$E_p = 30 \rightarrow 38$	150 \rightarrow 175	23.5519	-23.2078
$^{nat}\text{Zn}(p, x)^{66}\text{Ga}$	$E_p = 8 \rightarrow 12$	100 \rightarrow 120	—	—
$^{65}\text{Cu}(3\text{He}, 2n)^{66}\text{Ga}$	$E_{3\text{He}} = 12 \rightarrow 18$	150 \rightarrow 175	4.97152	-4.75084
$^{nat}\text{Cu}(3\text{He}, x)^{66}\text{Ga}$	$E_{3\text{He}} = 12 \rightarrow 18$	40 \rightarrow 50	—	—
$^{66}\text{Zn}(3\text{He}, x)^{66}\text{Ga}$	$E_{3\text{He}} = 24 \rightarrow 35$	300 \rightarrow 350	5.43119	-5.19359
$^{nat}\text{Zn}(3\text{He}, x)^{66}\text{Ga}$	$E_{3\text{He}} = 25 \rightarrow 33$	100 \rightarrow 120	—	—
$^{63}\text{Cu}(a, n)^{66}\text{Ga}$	$E_a = 12 \rightarrow 18$	300 \rightarrow 330	8.02538	-7.50165
$^{65}\text{Cu}(a, 3n)^{66}\text{Ga}$	$E_a = 35 \rightarrow 45$	250 \rightarrow 300	26.8899	-25.3285
$^{nat}\text{Cu}(a, x)^{66}\text{Ga}$	$E_a = 12 \rightarrow 18$	200 \rightarrow 240	—	—
$^{64}\text{Zn}(a, x)^{66}\text{Ga}$	$E_a = 26 \rightarrow 33$	600 \rightarrow 640	13.8039	-12.9905

and $^{64}\text{Zn}(a, x)^{66}\text{Ga}$, yielding 400-440 mb and 600-640 mb respectively, Shown in Table 1, These high yields make them especially attractive for practical production applications.

The threshold energies span a wide range from approximately 5 MeV to 27 MeV, with corresponding Q-values ranging from -4.75 to -25.33 MeV. Reactions involving natural targets (^{nat}Zn and ^{nat}Cu) do not have specific threshold energies and Q-values because of contributions from multiple isotopes. The optimal energy range has been carefully selected to maximize production yield while taking into account practical constraints, providing essential guidance for planning radioisotope production.

4. Conclusion:

The study presents the comprehensive investigation of the production routes of ^{66}Ga via proton, helium-3, and alpha-induced reactions on copper and zinc targets. The theoretical calculations by TALYS 1.9 were in general agreement with the experimental data providing valuable insights into reaction mechanisms. The most promising production paths were the $^{66}\text{Zn}(p, n)^{66}\text{Ga}$ and $^{64}\text{Zn}(a, x)^{66}\text{Ga}$ which show an optimum cross-section. Notably, ^{66}Ga production can be achieved with a small cyclotron due to the relatively low optimal energy ranges for most reactions, typically below 38 MeV. From the calculations in the study, it was found that the best projectiles that give good results for the cross sections are proton, helium-3 and alpha particles, as the results showed low energy ranges to achieve the cross section, and this is also supported by the practical results.

The compilation of threshold energies, Q-values, and optimal energy ranges constitutes a valuable resource for production planning and optimization, enabling efficient ^{66}Ga production for medical applications while minimizing unwanted by-products. Furthermore, the study explored the potential of natural target reactions, which, while exhibiting lower yields, offer cost-effective alternatives for certain applications. The findings of this research contribute significantly to the advancement of ^{66}Ga production methodologies, paving the way for its wider utilization in medical imaging and other relevant fields.

Funding: None.

Data Availability Statement: All of the data supporting the findings of the presented study are available from corresponding author on request.

Declarations: Conflict of interest: The authors declare that they have no conflict of interest.

Ethical approval: This research did not include any human subjects or animals, and as such, it was not necessary to obtain ethical approval.

References

- [1] S. M. Wong. *Introductory Nuclear Physics*. John Wiley Sons, Germany, 2^{ed} edition, 1998.

- [2] C.R. Chitambar. Medical applications and toxicities of gallium compounds. *International Journal of Environmental Research and Public Health*, 7: 2337–2361, 2010, doi:10.3390/ijerph7052337.
- [3] J. Kowalski, M. Henze, J. Schuhmacher, H.R. Mäcke, M. Hofmann, and U. Haberkorn. Evaluation of positron emission tomography imaging using [^{68}Ga]-DOTA-D Phe1-tyr3- octreotide in comparison to [^{111}In]-DTPAOC SPECT. *Molecular Imaging in Neuroendocrine Tumors*, 5(1): 42–48, 2003, doi:10.1016/S1536-1632(03)00038-6.
- [4] G.L. Griffiths, C.-H. Chang, W.J. McBride, E.A. Rossi, A. Sheerin, G.R. Tejada, H. Karacay, R.M. Sharkey, I.D. Horak, and H.J. Hansen. Reagents and methods for pet using bispecific antibody pretargeting and ^{68}Ga -radiolabeled bivalent hapten-peptide-chelate conjugates. *Journal of Nuclear Medicine*, 45: 30–39, 2004.
- [5] N.R.D.C. Network. Experimental nuclear reaction data (EXFOR/CSISRS). <https://www-nds.iaea.org/exfor/>, 2010.
- [6] Noori, Susan Shukur, A. Akkurt, and N.K. Demir. Excitation functions of proton induced reactions of some radioisotopes used in medicine. *Nutrients*, 16: 810–816, 2018, doi:10.1515/chem-2018-0085.
- [7] M. S. Alkhazraji, S. M. Aman Allah, and A. Ben Ahmed. Mott differential cross section by light nuclei using monte carlo simulation. *Indian Journal of Physics*, 98(4), 2023, doi:10.1007/s12648-023-02902-w.
- [8] E. Al-Sarray, S.S Noori, and S.A. Ebrahiem. Investigation of camel hair has a high ability to attenuate gamma rays. *AIP Conference Proceedings*, 2398: 020061, 2022, doi:10.1063/5.0097594.
- [9] N. K. Demir, B. Çetin, I. Akkurt, and S.S. Noori. Calculations of double differential cross sections on ^{56}Fe , ^{63}Cu and ^{90}Zr neutron emission in proton induced reactions. *Acta Physica Polonica A*, 132(3): 1181–1185, 2017, doi:10.12693/APhysPolA.132.1181.
- [10] N. Tuncel, S. S. Noori, N. Karpuz, M.I. Sayyed, and Iskender Akkurt. Proton, neutron and deuteron induced nuclear reactions in medical application. *Journal of Radiation Research and Applied Sciences*, 17(1): 100807, 2024, doi:10.1016/j.jrras.2023.100807.
- [11] Noori, Susan Shukur N. Karpuz, and I. Akkurt. Excitation functions of (d,n) reactions on some light nuclei. *Acta Physica Polonica A*, 129(1): 484–486, 2016, doi:10.12693/APhysPolA.130.484.
- [12] E. Tel, M. Sahan, A. Aydin, H. Sahan, F. A.Ugur, and A. Kapl. The newly calculations of production cross sections for some positron emitting and single photon emitting radioisotopes in proton cyclotrons. *Radioisotopes - Applications in Physical Sciences*, 2011, doi:10.5772/21109.
- [13] <https://nds.iaea.org/talys/>.
- [14] F. Szelecsényi, G.F. Steyn, Z. Kovács, T.N. Van Der Walt, K. Suzuki, K. Okada, and K. Mukai. New cross-section data for the $^{66}\text{Zn}(p,n)^{66}\text{Ga}$, $^{68}\text{Zn}(p,3n)^{66}\text{Ga}$, $^{nat}\text{Zn}(p,x)^{66}\text{Ga}$, $^{68}\text{Zn}(p,2n)^{67}\text{Ga}$ and $^{nat}\text{Zn}(p,x)^{67}\text{Ga}$ nuclear reactions up to 100 MeV. *Nuclear Instruments and Methods in Physics Research B*, 234: 375–386, 2005, doi:10.1016/j.nimb.2005.02.011.
- [15] F. Szelecsényi, Z. Kovács, T.N. Van Der Walt, G.F. Steyn, K. Suzuki, and K. Okada. Investigation of the $^{nat}\text{Zn}(p,x)^{62}\text{Zn}$ nuclear process up to 70 MeV: A new $^{62}\text{Zn}/^{62}\text{Cu}$ generator. *Applied Radiation and Isotopes*, 58: 377–384, 2003, doi:10.1016/S0969-8043(02)00345-7.
- [16] F. Szelecsényi, T.E. Boothe, S. Takács, F. Tárkányi, and E. Tavano. Evaluated cross section and thick target yield data bases of Zn + p processes for practical applications. *Applied Radiation and Isotopes*, 49(8): 129, 1998, doi:10.1016/S0969-8043(97)10103-8.
- [17] A. Hermanne, N. Walravens, and O. Cicchelli. Optimization of isotope production by cross section determination. *Nuclear Data for Science and Technology. Springer*, 13(4), 1992, doi:10.1007/978-3-642-58113-7_176.
- [18] V.N. Levkovski. *Cross Sections of Medium Mass Nuclide Activation (A= 40–100) by Medium Energy Protons and Alpha Particles (E= 10–50 MeV)*. Inter-Vesi, Moscow, USSR, 1991.
- [19] F. Tárkányi, F. Szelecsényi, Z. Kovács, and S. Sudár. Excitation functions of proton induced nuclear reactions on enriched ^{66}Zn , ^{67}Zn and ^{68}Zn . *Radiochim Acta*, 50(1-2): 19–26, 1990.
- [20] F.E. Little and M.C. Lagunas-Solar. Cyclotron production of ^{67}Ga . cross sections and thick-target yields for the $^{67}\text{Zn}(p,n)$ and $^{68}\text{Zn}(p,2n)$ reactions, journal = The International Journal of Applied Radiation and Isotopes, volume = 34(3), pages = 631–637, year = 1983, doi:10.1016/0020-708X(83)90067-4.
- [21] M. Hille, P. Hille, M. Uhl, and W. Weisz. Excitation functions of (p, n) and (α , n) reactions on Ni, Cu and Zn. *Nuclear Physics A*, 198: 625–640, 1972, doi:10.1016/0375-9474(72)90713-0.
- [22] H.A. Howe. (p,n) cross sections of copper and zinc. *Physical Review*, 109: 2083–2085, 1958, doi:10.1103/PhysRev.109.2083.
- [23] G. Pupillo, T. Sounalet, N. Michel, L. Mou, J. Esposito, and F. Haddad. New production cross sections for the theranostic radionuclide ^{67}Cu . *Nuclear Instruments Methods Physics Research B*, 415: 41–47, 2018, doi:10.1016/j.nimb.2017.10.022.
- [24] T. Stoll, S. Kastleiner, Y.N. Shubin, H.H. Coenen, and S.M. Qaim. Excitation functions of proton induced reactions on ^{68}Zn from threshold up to 71 MeV, with specific

- reference to the production of ^{67}Cu . *Radiochim. Acta*, 90: 309–313, 2002, doi:10.1524/ract.2002.90.6.309.
- [25] A. Hermanne, F. Szelecsényi, M. Sonck, S. Takács, F. Tárkányi, and P. Van Den Winkel. New cross section data on $^{68}\text{Zn}(p, 2n)^{67}\text{Ga}$ and $^{nat}\text{Zn}(p, xn)^{67}\text{Ga}$ nuclear reactions for the development of a reference data base. *Journal of Radioanalytical and Nuclear Chemistry*, 240(2): 623–630, 1999, doi:10.1007/BF02349423.
- [26] T. McGee, C.L. Rao, G.B. Saha, and L. Yaffe. Nuclear interactions of ^{45}Sc and ^{68}Zn with protons of medium energy. *Nuclear Physics A*, 150: 11–29, 1970, doi:10.1016/0375-9474(70)90451-3.
- [27] A.H. Asad, S. Chan, L. Morandau, D. Cryer, S. V. Smith, and R.I. Price. Excitation functions of $^{nat}\text{Zn}(p, x)$ nuclear reactions with proton beam energy below 18 MeV. *Applied Radiation and Isotopes*, 94: 67–71, 2014, doi:10.1016/j.apradiso.2014.07.008.
- [28] F.S. Al-Saleh, K.S. Al Mugren, and A. Azzam. Excitation function measurements and integral yields estimation for $^{nat}\text{Zn}(p, x)$ reactions at low energies. *Applied Radiation and Isotopes*, 65: 1101–1107, 2007.
- [29] M.S. Uddin, M.U. Khandaker, K.S. Kim, Y.S. Lee, and G.N. Kim. Excitation functions of the proton induced nuclear reactions on ^{nat}Zn up to 40 MeV. *Nuclear Instruments and Methods in Physics Research B*, 258: 313–320, 2007, doi:10.1016/j.nimb.2007.02.089.
- [30] F. Tárkányi, F. Ditrói, J. Csikai, S. Takács, M.S. Uddin, M. Hagiwara, M. Baba, Y.N. Shubin, and A.I. Dityuk. Activation cross-sections of long-lived products of proton-induced nuclear reactions on zinc. *Applied Radiation and Isotopes*, 62: 73–81, 2005, doi:10.1016/j.apradiso.2004.06.008.
- [31] M.L. Bonardi, F. Groppi, H.S. Mainardi, V.M. Kokhanyuk, E. V. Lapshina, M. V. Mebel, and B.L. Zhuikov. Cross section studies on ^{64}Cu with zinc target in the proton energy range from 141 down to 31 MeV. *Journal of Radioanalytical and Nuclear Chemistry*, 264(1): 101–105, 2005, doi:10.1007/s10967-005-0681-1.
- [32] P. Kopecký. Cross sections and production yields Ga for proton reactions in natural zinc. *The International Journal of Applied Radiation and Isotopes*, 41(6): 606–608, 1990, doi:10.1016/0883-2889(90)90048-L.
- [33] F.M. Nortier, S.J. Mills, and G.F. Steyn. Excitation functions and yields of relevance to the production of sup ^{67}Ga by proton bombardment of ^{nat}Zn and ^{nat}Ge up to 100 MeV. *Applied Radiation and Isotopes*, 42(2): 353–359, 1991, doi:10.1016/0883-2889(91)90138-Q.
- [34] M.C. Lagunas-Solar and R.P. Haff. Theoretical and experimental excitation functions for proton induced nuclear reactions on $Z = 10$ to $Z = 82$ target nuclides. *Radiochimica Acta*, 60: 57–68, 1993, doi:10.1016/0020-708X(83)90067-4.
- [35] P. Misaelides and H. Münzel. Excitation functions for ^3He - and α -induced reactions with ^{107}Ag and ^{109}Ag . *Journal of Inorganic and Nuclear Chemistry*, 42: 937–948, 1980, doi:10.1016/0022-1902(80)80379-4.
- [36] H.H. Bissem, R. Georgi, W. Scobel, J. Ernst, M. Kaba, J.R. Rao, and H. Strohe. Entrance and exit channel phenomena in d- and ^3He -induced preequilibrium decay. *Physical Review C*, 22(4): 1468–1484, 1980, doi:10.1103/PhysRevC.22.1468.
- [37] N.W. Golchert, J. Sedlet, and D.G. Gardner. Excitation functions for ^3He induced nuclear reactions in Cu. *Nuclear Physics A*, 152: 419–433, 1970, doi:10.1016/0375-9474(70)90842-0.
- [38] E.A. Bryant, D.R.F. Cochran, and J.D. Knight. Excitation functions of reactions of 7- to 24-MeV He^3 ions with Cu^{63} and Cu^{65} . *Physical Review*, 130: 1512–1522, 1963, doi:10.1103/PhysRev.130(4).1512.
- [39] E. Lebowitz and M.W. Greene. An auxiliary cyclotron beam monitor. *International Journal of Applied Radiation and Isotopes*, 21: 625–627, 1970, doi:10.1016/0020-708X(70)90106-7.
- [40] F. Tárkányi, F. Ditrói, S. Takács, M. Al-Abyad, M.G. Mustafa, Y. Shubin, and Y. Zhuang. New data and evaluation of ^3He -induced nuclear reactions on Cu. *Nuclear Instruments and Methods in Physics Research B*, 196: 215–227, 2002, doi:10.1016/S0168-583X(02)01286-7.
- [41] F. Tárkányi, F. Szelecsényi, and P. Kopecký. Cross section data for proton, ^3He and α -particle induced reactions on ^{nat}Ni , ^{nat}Cu and ^{nat}Ti for monitoring beam performance. In *Nuclear Data Science and Technology*. Springer, page 529–532, 1992.
- [42] Y. Nagame, H. Nakahara, and M. Furukawa. Excitation functions for ^3He particles induced reactions on Zinc. *Radiochim Acta*, 46: 5–12, 1989, doi:10.1524/ract.1989.46.1.5.
- [43] M. Al-Abyad, G.Y. Mohamed, F. Ditrói, S. Takács, and F. Tárkányi. Experimental study and nuclear model calculations of ^3He -induced nuclear reactions on zinc. *The european physical journal A.*, 53: 107–114, 2017, doi:10.1140/epja/i2017-12296-3.
- [44] A. Navin, V. Tripathi, Y. Blumenfeld, V. Nanal, C. Simenel, J.M. Casandjian, G. De France, R. Raabe, D. Bazin, and A. Chatterjee. Direct and compound reactions induced by unstable helium beams near the coulomb barrier. *Physical Review C.*, 70: 44601, 2004, doi:10.1103/PhysRevC.70.044601.
- [45] V.A. Didik, R.S. Malkovich, E.A. Skoryatina, and V. V. Kozlovskii. Experimental determination of the

- cross sections of nuclear reactions by the method of analysis of the concentration profiles of transmutation nuclides. *Atomic Energy*, 77(1): 570–572, 1994, doi:10.1007/BF02408219.
- [46] H.D. Bhardwaj, A.K. Gautam, and R. Prasad. Measurement and analysis of excitation functions for alpha-induced reactions in copper. *Pramana Journal of Physics*, 31(2): 109–123, 1988, doi:10.1007/BF02846965.
- [47] I.A. Rizvi, M.A. Ansari, R.P. Gautam, R.K.Y. Singn, and A.K. Chaubey. Excitation function studies of (α, xpyn) reactions for $^{63,65}\text{Cu}$ and pre-equilibrium effect. *Journal of the Physical Society of Japan*, 56(9): 3135–3144, 1987, doi:10.1143/JPSJ.56.3135.
- [48] J. Zweit, H. Sharma, and S. Downey. International journal radiation applications and instrumentation. *Applied Radiation and Isotopes*, 38(7): 499–501, 1987, doi:10.1016/0883-2889(87)90194-8.
- [49] P. H. Stelson and F. K. McGowan. Cross sections for (α, n) reactions for medium-weight nuclei. *Physical Review*, 133(4B): 911–919, 1964, doi:10.1103/PhysRev.133.B911.
- [50] Murat ÖNAL and Halime ÇALI ÖZTÜRK. Crosschecking of alpha particle monitor reactions up to 50 MeV. *Nuclear Instruments and Methods in Physics Research B*, 397: 33–38, 2017, doi:10.1016/j.nimb.2017.02.033.
- [51] K.G. Porges. Alpha excitation functions of silver and copper. *Physical Review*, 101(1): 225–230, 1956, doi:10.1103/PhysRev.101.225.
- [52] A.R. Usman, M.U. Khandaker, H. Haba, N. Otuka, M. Murakami, and Y. Komori. Production cross-sections of radionuclides from α -induced reactions on natural copper up to 50 MeV. *Applied Radiation and Isotopes*, 114: 104–113, 2016, doi:10.1016/j.apradiso.2016.04.027.
- [53] M. Shahid, K. Kim, G. Kim, M. Zaman, and M. Nadeem. Measurement of excitation functions in alpha induced reactions on ^{nat}Cu . *Nuclear Instruments and Methods in Physics Research B.*, 358: 160–167, 2015, doi:10.1016/j.nimb.2015.06.026.
- [54] F. Szelecsényi, Z. Kovács, K. Nagatsu, K. Fukumura, K. Suzuki, and K. Mukai. Investigation of direct production of ^{68}Ga with low energy multiparticle accelerator. *Radiochim Acta*, 100: 5–11, 2012, doi:10.1524/ract.2011.1896.
- [55] F. Szelecsényi, K. Suzuki, Z. Kovács, M. Takei, and K. Okada. Alpha beam monitoring via ^{nat}Cu + alpha processes in the energy range from 40 to 60 MeV. *Nuclear Instruments and Methods in Physics Research B*, 184: 589–596, 2001, doi:10.1016/S0168-583X(01)00793-5.
- [56] F. Tárkányi, F. Szelecsényi, S. Takács, A. Hermanne, M. Sonck, A. Thielemans, M.G. Mustafa, Y. Shubin, and Z. Youxiang. New experimental data, compilation and evaluation for the $^{nat}\text{Cu}(\alpha, x)^{66}\text{Ga}$, $^{nat}\text{Cu}(\alpha, x)^{67}\text{Ga}$ and $^{nat}\text{Cu}(\alpha, x)^{67}\text{Zn}$ monitor reactions. *Nuclear Instruments Methods Physics Research B*, 168: 144–168, 2000, doi:10.1016/S0168-583X(99)00877-0.
- [57] M. Sonck, J. Van Hoyweghen, and A. Hermanne. Determination of the external beam energy of a variable energy multiparticle cyclotron. *Applied Radiation and Isotopes*, 47(4): 445–449, 1996, doi:10.1016/0969-8043(95)00323-1.
- [58] S. Mirzadeh and Y. Y. Chu. Production of gallium-66, a positron emitting nuclide for radioimmunotherapy. In *Nuclear Data for Science and Technology*, page 619–621, 1991, doi:10.1007/978-3-642-58113-7_77.

تحسين إنتاجية ^{66}Ga : تقييم طرق الإنتاج عبر قصف نظائر النحاس والزنك بالبروتون، الهيليوم -3 وجسيمات ألفا

سوزان شكر نوري *

قسم الفيزياء، كلية العلوم، جامعة كركوك، كركوك، العراق.

* الباحث المسؤل: susannoori@uokirkuk.edu.iq

الخلاصة

تلعب النويدات المشعة متوسطة العمر جاليوم -66 (عمر النصف $T_{1/2} = 9.5$ ساعة، $\beta^+ = 56\%$ ، $\epsilon = 45\%$) دورًا مهمًا في التصوير المقطعي بالإصدار البوزيتروني (PET). تقدم هذه الدراسة تحليلًا شاملاً لاثني عشر مسارًا مختلفًا للتفاعل النووي لإنتاج جاليوم -66 مع اختبار قصف البروتون والهيليوم -3 وجسيمات ألفا على أهداف من النحاس والزنك. تم حساب المقاطع العرضية باستخدام كود محاكاة التفاعل النووي TALYS1.9 للتفاعلات $^{66}\text{Zn}(p,n)^{66}\text{Ga}$ ، $^{67}\text{Zn}(p,2n)^{66}\text{Ga}$ ، $^{68}\text{Zn}(p,3n)^{66}\text{Ga}$ ، $^{66}\text{Zn}(^3\text{He},x)^{66}\text{Ga}$ ، $^{nat}\text{Zn}(^3\text{He},x)^{66}\text{Ga}$ ، $^{65}\text{Cu}(^3\text{He},2n)^{66}\text{Ga}$ ، $^{nat}\text{Zn}(p,x)^{66}\text{Ga}$ ، $^{63}\text{Cu}(a,n)^{66}\text{Ga}$ ، $^{64}\text{Zn}(a,x)^{66}\text{Ga}$ و $^{nat}\text{Cu}(a,x)^{66}\text{Ga}$ ، $^{65}\text{Cu}(a,3n)^{66}\text{Ga}$ ، ^{65}Cu ، ^{nat}Cu ، ^{64}Zn ، ^{66}Zn ، ^{67}Zn و ^{68}Zn ، تم التحقق من صحة الحسابات النظرية بالمقارنة مع البيانات التجريبية من مكتبة EXFOR. والجدير بالذكر أن التفاعلات $^{66}\text{Zn}(p,n)^{66}\text{Ga}$ و $^{64}\text{Zn}(a,x)^{66}\text{Ga}$ أظهرت كفاءة استثنائية، حيث حققت مقاطع عرضية قصوى تبلغ 440-400 ميجابايت و 640-600 ميجابايت على التوالي. تم تحديد نطاقات الطاقة المثلى، طاقات العتبة وقيم Q لكل مسار تفاعل من التفاعلات قيد الدراسة مما يوفر معلمات أساسية لتحسين إنتاج جاليوم -66 للاستخدام في التطبيقات الطبية.

الكلمات الدالة: إنتاج الجاليوم -66؛ المقاطع العرضية النووية؛ حسابات TALYS؛ إنتاج النظائر الطبية؛ نظائر التصوير المقطعي بالإصدار البوزيتروني.

التمويل: لا يوجد.

بيان توفر البيانات: جميع البيانات الداعمة لنتائج الدراسة المقدمة يمكن طلبها من المؤلف المسؤل.

اقرارات:

تضارب المصالح: يقر المؤلفون أنه ليس لديهم تضارب في المصالح.

الموافقة الأخلاقية: لم يتضمن هذا البحث أي تجارب على البشر أو الحيوانات، بالتالي لم يكن من الضروري الحصول على موافقة أخلاقية.